



SACRED HEART RESEARCH PUBLICATIONS

Journal of Functional Materials and Biomolecules

Journal homepage: www.shcpub.edu.in



ISSN: 2456-9429

Spectral investigation of aminoacid modified DNA self-assembled magnetite Fe₃O₄ nanoparticles

Kalaimani Narayana Boopathi^{1,3}, A. Manivel⁴, Natarajan Prabakaran^{1,2*}

Received on 15 September 2020, accepted on 17 December 2020,

Published online on 31 December 2020

Abstract

The core-shell modification of Fe₃O₄ based magnetic nanoparticles (MNPs) with amino acid (i.e L-Alanine; L-Methionine; L-Cysteine) functionalised DNA self-assembled structure was studied. Biocompatible core-shell MNPs were prepared with an average of 60-70 nm. The sonochemical method was employed to successful modification were attempt. The structure and properties of sample were characterised using X-ray diffraction, Fourier transform infra-red (FT-IR) spectroscopy, Scanning electron microscopy (SEM), Vibrating sample magnetometer (VSM), UV-vis spectroscopy, Atomic force microscopy (AFM) and Transmission electron microscopy (TEM). The VSM results show the 8.04 emu g⁻¹. The FT-IR shows the 2550–2650 cm⁻¹ (νS-H) for L-cysteine disappears, which indicates that the sulphur atom in mercapto group is coordinated with Fe³⁺/Fe²⁺ ions on the surface of the magnetic nanoparticles. The UV-vis and AFM reveals the self-assembled structure.

Keywords: Biocompatible, self-assembled, Aminoacid functionalised MNPs, DNA self-assembled NPs.

1 Introduction

Magnetic nanoparticles (MNPs) have recently undergone intensive research because of their suitable properties for a diverse set of potential applications in biomedicine, catalysis, etc. [1–9] At the nanoscale, magnetic materials display novel physical effects that distinguish them from their bulk counterparts. This phenomenon is known as nanomagnetism, and it endows MNPs with unique properties such as superparamagnetism. It should be noted that well-defined nanostructures in MNPs are critical to achieve these unique properties. However, great challenges remain in obtaining monodisperse magnetic nanostructures because of the dipolar interactions and surface effects of MNPs at the nanoscale, as well as in addressing the control of grains, antioxidation, etc. With the controlled synthesis and proper modification, these nanocomposites can exhibit novel physical and chemical properties that will be essential for biomedical applications, especially the highly sensitive and selective sensors and separators. [10–13]. Nanomedicine has been employed as a developmental treatment for an illness that is difficult to conquer in clinical medicine, such as breast cancer. Nanoparticles bear identical properties, including the enhanced

permeability and retention (EPR) effect, for anticancer nanomedicine targeting, accurate drug delivery to tumor tissues, and controlled drug release at the disease sites. [14–19] Codelivery of anticancer drugs using different nanoscales and functional nanocarriers has shown capabilities for improving drug targeting delivery and therapeutic efficacies while limiting the toxicity of drug by its targeting and controlled release only around cancer cells. [14,15,20]

Many research groups synthesized magnetite nanocrystal clusters with various sizes through thermal decomposition of iron(III) chloride in ethylene glycol with addition of different substances such as sodium and ammoniumacetate, polyethyleneglycol, ethylenediaminesodiumcitrate, poly(acrylic acid), urea, [21–23] and microclusters. [24–26] Derivatives of carboxylic, sulfonic, phosphoric, and phosphonic acids bind to the MNP surface via non-covalent absorption and allow to obtain stable colloidal solutions of MNPs in aqueous media. Unlike carboxylic acids, there are not many published examples of using phosphonic or phosphoric acid derivatives, although they can be successfully applied to provide a hydrophilic, biocompatible, and biodegradable coating on MNPs. [27] To purpose of this study the surface modification of Fe₃O₄ MNPs (obtained from precipitation from the solution of Fe³⁺ and Fe²⁺ salts) with biocompatible aminoacid such as L-alanine, L-cysteine and L-methionine and study their magnetic contrast properties and self-assembled DNA-magnetite in experiments, we believe will be useful in the development of MRI contrast agents including those for diagnostics.

2 Experimental

2.1 Reagents and Materials.

Ferrous sulphate dihydrate (FeSO₄ · 2H₂O; Merck) Ferric chloride (FeCl₃; Merck) was used as Iron precursor. Cetyltrimethylammonium bromide (CTAB; Merck), citric acid and oleic acid monohydrate (Sigma-Aldrich) were used as stabilizers. Liq ammonia (Merck) was used as a reducing

*Corresponding author: e-mail an.prabakar@gmail.com

¹School of Chemistry, Madurai Kamaraj University, Madurai-625021

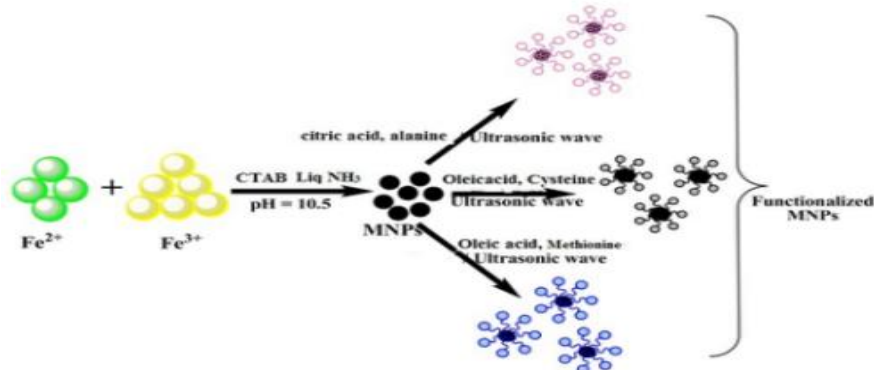
²Department of Chemistry, Yadava College, Madurai-625014

³P.G. Assistant in Chemistry, Govt. Hr. Sec. School, Thaniyamangalam, Madurai-625109.

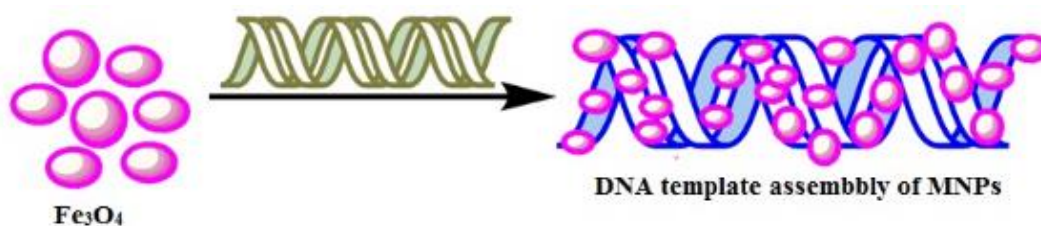
⁴P.G. and Research Department, Saraswathi Narayanan College, Perungudi, Madurai-625022

reagent. L-Alanine, L-cysteine (Loba) and L-Methionine (SRL) was used for surface functionalized aminoacids. All chemicals were of analytical grade and were used as received. Herring sperm DNA (Sisco research laboratory, India) were used for the Fe₃O₄-DNA template self-

assembled method. Tris-Hcl, acetic acid and sodium hydroxide were used for Tris- buffer preparation. Ultrapure double distilled water was used in all the preparations and was deaerated by bubbling with N₂ gas for 30 min prior to the preparation of aqueous solutions of precursor of iron.



Scheme 1



Scheme 2

2.2 Preparation of Fe₃O₄ nanoparticles.

The procedure slightly modified from the method reported by P. Sharma et al [28] is adopted for the preparation of Fe₃O₄ nanoparticles. Accordingly, 5 ml of 4M citric acid were dissolved in 100 mL of 0.1% solution of CTAB in deoxygenated water (nitrogen gas sparingly); and 2:1 weight ratio of the 1.2 g of FeCl₃ and 0.6 g of FeSO₄. 2H₂O were successively dissolved in the solution with vigorous stirring. The resulting solution was added drop wise into 100 mL of liq. NH₃ solution under stirring. The black precipitate was generated as the pH reached the 10. The fine powder of the precipitate was made to settle using the external magnetic field and the supernatant was decanted. Purified deoxygenated water was added to the black mass with stirring and centrifuged at 6000 rpm. After repeating the last step more than 5 times the pH was adjusted to neutral by adding 0.01 M HCl. Finally, the black magnetic nanoparticles (MNPs) were washed in acetone and separated using magnet and then dried.

2.3 Preparation of aminoacid modified Fe₃O₄/γ-Fe₂O₃ nanoparticles.

The modified procedure [29] described in scheme 1 was used to aminoacid modified magnetic nanoparticles (MNPs). 100 mg of Fe₃O₄ magnetic nanoparticles (MNPs) were dispersed in 30 mL of hexane using sonication for 30 min. 600 μL of oleic acid/citric acid solution were added to the suspension and were sonicated for 30 min and then followed by the addition of 10 mL of 1 mmol of amino acid

(i.e L-Alanine; L-Methionine; L-Cysteine) was added to continue the reflux another 3 h. After that the core-shell modified aminoacid MNPs fine powder were obtained to evaporate to dry used as further characterization.

2.4 Preparation of Template assembly of DNA with MNPs.

The 2:1 ratio of the herring sperm DNA and Fe₃O₄ magnetic nanoparticles and aminoacid functionalised (Fe₃O₄@L-Ala/L-Cys/L-Methio) MNPs mixture were incubated in the Tris. HCl buffer at 45 min at room temperature and then stirred over 3h and then added to the ethanol to the above solution. The aggregate precipitate was settled to use 6000 rpm and then dispersed to the buffer to the further studies [30-31].

2.5 Characterization.

The Fe₃O₄ magnetic nanoparticles (MNPs), core-shell modified aminoacid MNPs fine powder and template DNA-MNPs were characterized by XRD, FT-IR spectroscopy, scanning electron microscopy (SEM), transmission electron microscopy (TEM), UV-vis spectroscopy, and atomic force microscopy (AFM). The X-ray powder pattern for the crystalline nature of nanostructured complexes were recorded by a XPERT-PRO Diffractometer using Cu Kα radiation ($\lambda = 1.54060 \text{ \AA}$) with Ni filter in a 2θ range. FT-IR spectra were measured with a Shimadzu FT-IR-8400s (4000-400 cm⁻¹) spectrophotometer. SEM images were recorded using a Hitachi S-3400 scanning electron micro-

scope operating at 20 kV. TEM images were performed with a JEOL 3011 transmission electron microscope operating at 200 kV. Samples for TEM were prepared by dropping and evaporating the nanoparticle suspensions on a copper grid under nitrogen atmosphere. Samples for SEM and AFM were prepared by dropping and evaporating the nanoparticle colloids on a glass plate. AFM analysis was performed using AFM A100 SGS scanning probe microscope. The interactions of these nanoparticles with herring sperm DNA were studied through UV-vis absorption spectra were measured with a Jasco J-550 spectrophotometer and AFM A100 SGS scanning probe microscope.

3 Results and Discussion

3.1 FT-IR spectra:

The Fourier Transform infrared spectrum (FT-IR) Fe_3O_4 and amino acid functionalised ($\text{Fe}_3\text{O}_4@L\text{-Ala}/L\text{-Cys}/L\text{-Methio}$) magnetic nanoparticles were examined in Figure 1 and 2. As is known for free amino acids, which exhibit the broad band upon 3400 cm^{-1} in the region of the -NH stretching vibrations, while the -C=O ($\nu(\text{CO})$) stretching vibrations display in the region of 1600 cm^{-1} .

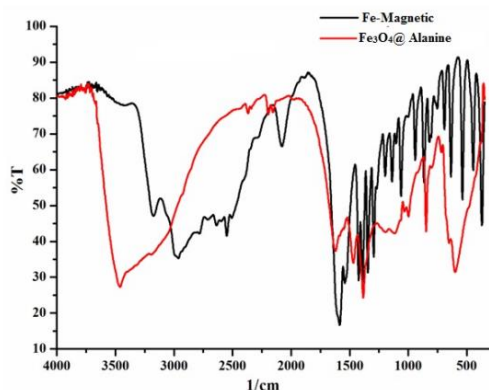


Figure 1. FTIR spectra of magnetic Fe_3O_4 and $\text{Fe}_3\text{O}_4@L\text{-Ala}$ nanoparticles.

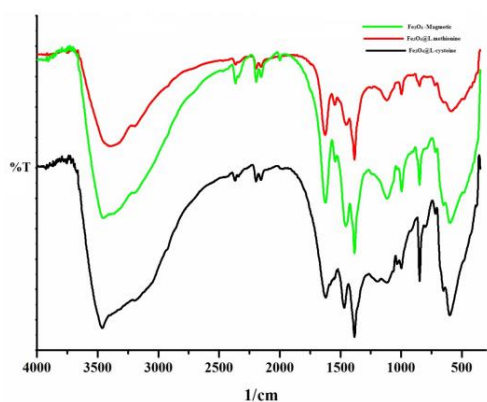


Figure 2. FTIR spectra of $\text{Fe}_3\text{O}_4@L\text{-Ala}/L\text{-Cys}/L\text{-Methio}$ magnetic nanoparticles.

Figure 1 and 2 shows the Fe_3O_4 and amino acid functionalised magnetic nanoparticles ($\text{Fe}_3\text{O}_4@L\text{-Ala}/L\text{-Cys}/L\text{-Methio}$) ν : $1550\text{--}1650\text{ cm}^{-1}$ ($\text{s } \nu\text{C-O}$), 1394 cm^{-1} ($\text{m } \nu\text{C-O}$), $1200\text{--}1250\text{ cm}^{-1}$ ($\text{w } \nu\text{C=O}$), $3500\text{--}3000\text{ cm}^{-1}$ ($\text{m } \nu\text{O-H}$), $2900\text{--}3420\text{ cm}^{-1}$ ($\text{m } \nu\text{N-H}$), 1068 cm^{-1} ($\text{m } \nu\text{C-NH}_2$) and $600\text{--}800\text{ cm}^{-1}$ ($\text{w } \nu\text{C-S}$) were found, while the $2550\text{--}2650\text{ cm}^{-1}$ ($\nu\text{S-H}$) for L-cysteine [32-33] disappears, which in-

dicates that the sulfur atom in mercapto group of L-cysteine and L-methionine is coordinated with $\text{Fe}^{3+}/\text{Fe}^{2+}$ ions on the surface of the magnetic nanoparticles, resulting in the formation of $\text{Fe}_3\text{O}_4@L\text{-Ala}/L\text{-Cys}/L\text{-Methio}$ nanocluster. The peaks at 586 and 631 cm^{-1} were related to a Fe-O stretching vibration derived from the splitting of the band at 570 cm^{-1} which indicates the existence of Fe_3O_4 in the core-shell [34].

3.2 VSM study:

From the vibrating sample magneto metric measurements (VSM), the saturation of magnetization (M_s) of Fe_3O_4 nanoparticles and oleic with methionine functionalised Fe_3O_4 nanoparticles were found to be 8.04 emu g^{-1} respectively, at 300 K (Figure 3). This sample consists of magnetic nanoparticles with an average size from 26 to 32 nm (From SEM). As earlier reported a saturation magnetization value of 15 emu g^{-1} for Fe_3O_4 nanoparticles with 2 nm thickness with silica [35] is known, the saturation magnetization values for silica coated Fe_3O_4 nanoparticles are generally below 5 emu g^{-1} [36,37]. From this observation the present observed saturation magnetization value of 8.64 emu g^{-1} clearly suggest the formation L-methionine with oleic acid can be encapsulated with good interaction between the Fe_3O_4 MNPS. The saturation magnetization Fe_3O_4 nanoparticles and coating decreases the magnetization value and because of this the functionalised Fe_3O_4 nanoparticles will find its way in future as a tool for drug delivery applications.

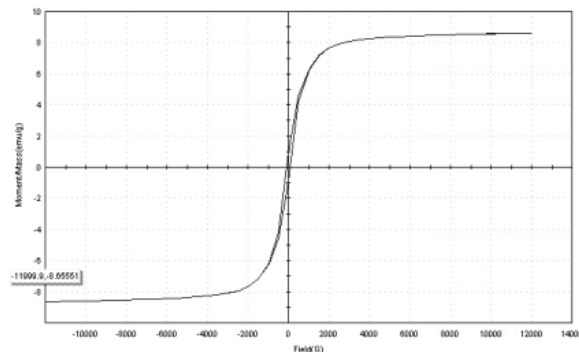


Figure 3. Plot of magnetization versus magnetic field for Fe_3O_4 nanoparticles.

3.3. Structural analysis:

3.3. 1 XRD

The phase purity and chemical composition of the magnetic nanoparticles (MNPs) of Fe_3O_4 and amino acid functionalised ($\text{Fe}_3\text{O}_4@L\text{-Ala}/L\text{-Cys}/L\text{-Methio}$) MNPs were examined by XRD. The Diffraction peaks shown in Figure 4 could be assigned to Fe_3O_4 phase according to Joint Committee on Powder Diffraction Standards (JCPDS), observed in the selected area diffraction pattern of the Fe_3O_4 and amino acid functionalization ($\text{Fe}_3\text{O}_4@L\text{-Ala}/L\text{-Cys}/L\text{-Methio}$) MNPS. The peak can be indexed at 35.10 , 41.41 , 43.35 , 50.48 , 62.97 , 67.28 , and 74.18 (JCPDS-no 19-0629; 85-1436) indicating that the cores of these MNPs have a cubic inverse spinel structure [38] with the reflection planes (122), (311), (222), (400), (422), (511) and (444). The average size of Fe_3O_4 and amino acid function-

alization ($\text{Fe}_3\text{O}_4@L\text{-Ala}/L\text{-Cys}/L\text{-Methio}$) MNPS were found to be about 32 to 41 nm.

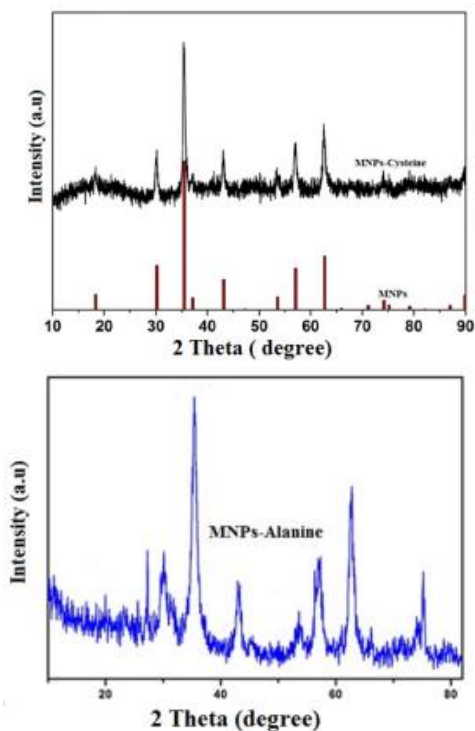


Figure 4. Powder XRD pattern of the Fe_3O_4 and amino acid functionalised ($\text{Fe}_3\text{O}_4@L\text{-Ala}/L\text{-Cys}$) MNPS

3.3.2. SEM and TEM:

Figure 5 shows the SEM image of the amino acid functionalisation ($\text{Fe}_3\text{O}_4@L\text{-Ala}/L\text{-Cys}$) MNPS. It is clear that the particles are in the size range of 60-70 nm. Fig. 5c shows the magnified SEM images of the amino acid functionalisation L-cys @ Fe_3O_4 nanoparticles prepared in water dispersion. The amino acid functionalised MNPs exhibit neatly assembled with cluster in nature. L-Alanine and L-cysteine functionalised MNPs uniform in size and are shown in the spherical aggregated cluster around 100 to 200 nm which on magnified image are confirmed the uniform distribution.

TEM image of Fe_3O_4 magnetic nanoparticles and amino acid functionalised ($\text{Fe}_3\text{O}_4@L\text{-Ala}/L\text{-Cys}/L\text{-Methio}$) MNPs are shown in Figure 6 and 7. It shows the core-shell structure of Fe_3O_4 magnetic nanoparticles of about 30 nm in size (Figure 6b). This core-shell morphology of the Fe_3O_4 magnetic nanoparticles was retained even after functionalisation with L-Alanine/L-Cysteine/L-Methionine with a second shell formation over the existing one (Figure 7). However, during Fe_3O_4 functionalisation, core dissolution or oxidation was observed in the form of aggregation. In order to demonstrate whether there is any size increment due to functionalisation, particle sizes were measured before and after the functionalisation [29,30]. The overall size of the iron oxide particles is about increase in 15 nm and the size of $\text{Fe}_3\text{O}_4@L\text{-Ala}/L\text{-Cys}/L\text{-Methio}$ after the coating went up to 40 - 50 nm, which clearly indicates the presence of additional materials around Fe_3O_4 .

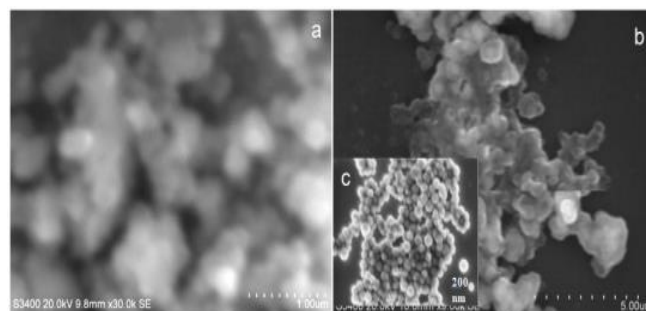


Figure 5. Scanning electron microscopy (SEM) images of amino acid functionalized (a) magnetite NP in alanine; and (b) magnetite NP in L-Cysteine inset c shows the magnification of the L-cys @ Fe_3O_4

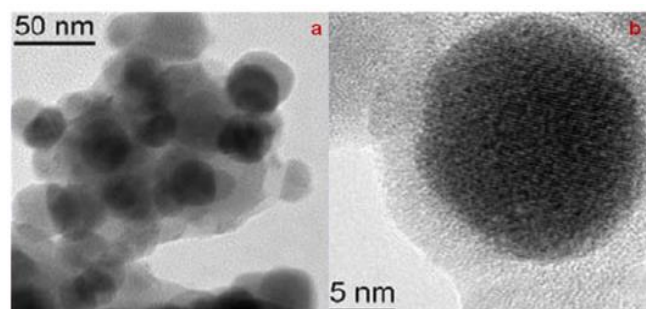


Figure 6. Transmission electron microscopy (TEM) images of (a) magnetite NP in CTAB(cetyl trimethyl ammonium bromide) ; (b) High resolution transmission electron microscopy (HRTEM) images of magnetite NPs embedded in a CTAB matrix

3.4 Self-assembled DNA@MNPs.

3.4.1 Electronic spectra

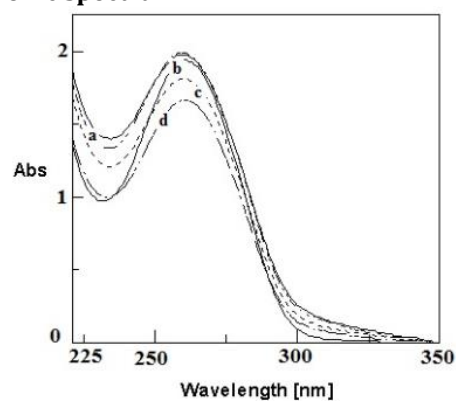


Figure 8. Fe_3O_4 magnetic nanoparticles and amino acid functionalised ($\text{Fe}_3\text{O}_4@L\text{-Ala}/L\text{-Cys}/L\text{-Methio}$) MNPs with DNA (a- Fe_3O_4 ; b- $\text{Fe}_3\text{O}_4@L\text{-Ala}$; c- $\text{Fe}_3\text{O}_4@L\text{-Cys}$; d- $\text{Fe}_3\text{O}_4@L\text{-Methio}$)

The Fe_3O_4 magnetic nanoparticles and amino acid functionalised ($\text{Fe}_3\text{O}_4@L\text{-Ala}/L\text{-Cys}/L\text{-Methio}$) MNPs were dispersed in water and then interacted with herring sperm DNA. In order to check the interaction of Fe_3O_4 magnetic

nanoparticles and amino acid functionalised ($\text{Fe}_3\text{O}_4@L\text{-Ala}/L\text{-Cys}/L\text{-Methio}$) MNPs with DNA [30,31,39], the micro molar solution of DNA was treated with 20 mg of Fe_3O_4 magnetic nanoparticles and amino acid functionalised ($\text{Fe}_3\text{O}_4@L\text{-Ala}/L\text{-Cys}/L\text{-Methio}$) MNPs. The absorption values decreased with hypochromism were observed (Figure 8) and slightly red shift around 2-8 nm (from Table-1 supporting information). The Fe_3O_4 magnetic nanoparticles and amino acid functionalised ($\text{Fe}_3\text{O}_4@L\text{-Ala}/L\text{-Cys}/L\text{-Methio}$) MNPs interaction with a negatively charged phosphate backbone of DNA may be considered as electrostatic mode.

3.4.2 AFM

Atomic Force Microscope was used to characterize the DNA with Fe_3O_4 and amino acid functionalised ($\text{Fe}_3\text{O}_4@L\text{-Ala}/L\text{-Cys}/L\text{-Methio}$) MNPs.

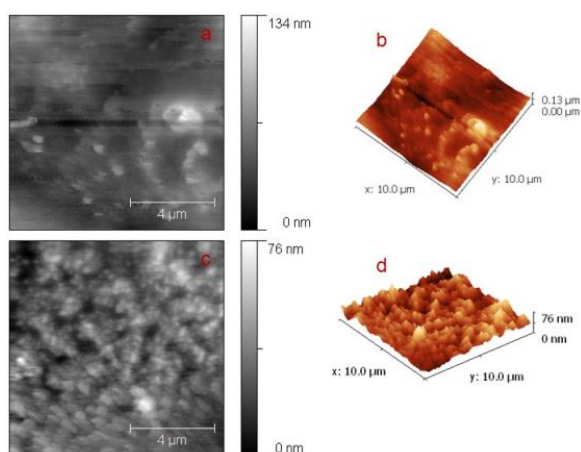


Figure 9. The AFM image under solution for (a) DNA with Fe_3O_4 magnetic nanoparticles, (b) 3D image of a, (c) DNA with $\text{Fe}_3\text{O}_4@L\text{-Methio}$ MNPs and (d) 3D image of c.

Dilute samples were imaged on ultra thin film coated over the electron microscope cover slip in polymeric material with lysine solution (5mg per mL) to enhance the binding of the oligonucleotide. Experiments using a double stranded oligonucleotide with Fe_3O_4 magnetic nanoparticles and amino acid functionalised $\text{Fe}_3\text{O}_4@L\text{-Methio}$ MNPs control showed that the more than 70% of the MNPs are well impregnated to the adsorption and well binded, thereby excluding the possibility of aggregation to AFM sample preparation.

At molecular level, the AFM image of DNA-Fe MNPs and $\text{Fe}_3\text{O}_4@L\text{-Methio}$ MNPs (Figure 9) were consistent with the expected dimeric structure. The overall topology of the stable, rigid twisted twine bundles of the helix are observed, particularly attractive for building programmable architecture modeling of the parallel and anti parallel dimmers. The functionalised $\text{Fe}_3\text{O}_4@L\text{-Methio}$ MNPs were well arranged on the superimposable [29,30,39] of the DNA but Fe MNPs are formed in the aggregated dimeric cluster in regular and irregular fashion due to strong interaction in the $\text{Fe}^{2+}/\text{Fe}^{3+}$ MNPs. The distance observed under the AFM for parallel and anti parallel ranges from 76 and 134 nm respectively. As an evident for that the fab-

rication of MNPs with functionalized MNPs ability to chemically controllable for template synthesis of DNA assembly.

4 Conclusion

In this study, reveals the surface functionalised MNPs were synthesis using hydro and solvothermal method. The modified MNPs have good colloidal and magnetic stability. The functionalised MNPs were assisted to the biocompatible of DNA to form a self-assembled edifice. In future, it's helpful to design a multimodal agent for biomedical applications of targeted drug delivery system.

Acknowledgement

The author thanks to Prof. A. Ponnusamy, Prof and Head, Department of Organic Chemistry, SOC, MKU and Dr. S. Murugesan, Department of Inorganic Chemistry, SOC, MKU for valuable helps and allowed to permit in the work of his laboratories. In addition to that, thanks to my Headmaster, DEO and CEO granting permission to gain a knowledge of updating to complete my M.Phil., degree.

References

- [1] R. Hao, R. Xing, Z. Xu, Y. Hou, S. Gao and S. Sun, *Adv. Mater.* 22 (2010) 2729–2742.
- [2] F. Liu, Y. Hou and S. Gao, *Chem. Soc. Rev.* 43 (2014) 8098–113.
- [3] L. Wu, A. Mendoza-Garcia, Q. Li and S. Sun, *Chem. Rev.* 116 (2016) 10473–10512.
- [4] R. Scarfiello, C. Nobile and P. D. Cozzoli, *Front. Mater.* 3 (2016) 56.
- [5] Y. Hou and D. Sellmyer, *Magnetic Nanomaterials: Fundamentals, Synthesis and Applications*; J., Eds.; Wiley-VCH: Weinheim, Germany, (2017).
- [6] R. B. Nasir Baig, M. N. Nadagouda and R. S Varma, *Coord. Chem. Rev.* 287 (2015) 137–156.
- [7] V. K. LaMer and R. H. Dinegar, *J. Am. Chem. Soc.* 72 (1950) 4847–4854.
- [8] B. R. Smith and S. S. Gambhir, *Chem. Rev.* 117 (2017) 901–986.
- [9] K. Ulbrich, K. Holá, V. Šubr, A. Bakandritsos, J. Tuček and R. Zbořil, *Chem. Rev.* 116 (2016) 5338–5431.
- [10] N. Agnihotri, A. D. Chowdhury and A. De, *Biosens. Bioelectron.* 63 (2015) 212–217.
- [11] A. D. Chowdhury, A. De, C. R. Chaudhuri, K. Bandyopadhyay and P. Sen, *Sens. Actuators, B* 172 (2012) 916–923.
- [12] Z. Zhu, J. J. Lu and S. Liu, *Anal. Chim. Acta* 709 (2012), 21–31.
- [13] A. D. Chowdhury, N.; Agnihotri, A. De and M. Sarkar, *Sens. Actuators, B* 202 (2014) 917–923.
- [14] X. Li, M. Takashima, E. Yuba, A. Harada and K. Kono, *Biomaterials* 35 (2014) 6576–6584.
- [15] A. Eldar-Boock, D. Polyak, A. Scomparin and R. Satchi-Fainaro, *Curr. Opin. Biotechnol.* 24 (2013) 682–689.
- [16] G. Y. Lee, J. H. Kim, K. Y. Choi, H. Y. Yoon, K. Kim and I. C. Kwon, *Biomaterials* 53 (2015) 341–348.

- [17] T. Thambi, V. Deepagan, H. Y. Yoon and H. S. Han, *Biomaterials* 35 (2014) 1735–1743.
- [18] H. Y. Yoon, H. Koo, K. Y. Choi, I. C. Kwon, K. Choi and J. H. Park, *Biomaterials* 4 (2013) 5273–5280.
- [19] E. Ju, Z. Liu, Y. Du, Y. Tao, J. Ren and X. Qu, *ACS Nano* 8 (2014) 6014–6023.
- [20] F. Li, X. Zhao, H. Wang, R. Zhao, T. Ji, H. Ren, G. J. Anderson, G. Nie and J. Hao, *Adv. Funct. Mater.* 25 (2015) 788–798.
- [21] K. C. Barick, M. Lin, Y.-P. Aslam, D. Bahadur, P. V. Prasad and V. P. Dravid, *J. Mater. Chem.* 19 (2009) 7023-7029.
- [22] M. Li, H. Gu and C. Zhang, *Nanoscale Res. Lett.* 7 (2012) 204-214.
- [23] F. Dong, W. Guo, J. H. Bae, S. H. Kim and C. S. Ha, *Chem. - Eur. J.* 17 (2011) 12802–12808.
- [24] H. Deng, X. Li, Q. Peng, X. Wang, J. Chen and Y. Li, *Angew. Chem., Int. Ed.* 44 (2005) 2782–2785.
- [25] S.; Xuan, Y.-X. J.; Wang, J. C.; Yu and K. Cham-Fai Leung, *Chem. Mater.* 21 (2009) 5079–5087.
- [26] T. Fan, D. Pan and H. Zhang, *Ind. Eng. Chem. Res.* 50 (2011) 9009–9018.
- [27] J. Galezowska and E. Gumienna-Kontecka, *Coord. Chem. Rev.* 256 (2012) 105–124.
- [28] P. Sharma, S. Rana, K. C. Barick, C. Kumar, H. G. Salunke and P. A. Hassan, *New J. Chem.* 38 (2014) 5500–5508.
- [29] A. Pershina, A. Demin, V. Ivanov, K. Nevskaya, O. Shevelev, A. Minin, I. Byzov, A. Sazonov, V. Krasnov and L. Ogorodova, *Int. J. Nanomed.* 11 (2016) 4451–4463.
- [30] N. C. Seeman, *Angew. Chem. Int. Edn Engl.* 37, (1998) 3220–3238.
- [31] A. M.; Demin, A. V.; Mekhaev, A. A.; Esin, D. K.; Kuznetsov, P. S.; Zelenovskiy, V. Y. Shur and V. P. Krasnov, *Appl. Surf. Sci.* 440 (2018) 1196–1203.
- [32] Mohapatra, S.; Pramanik, P. *Colloids Surf., A* 2009, 339, 35–42.
- [33] R. D. Waldron, *Phys. Rev.* 99 (1955) 1727–1735.
- [34] G. K. Kouassi, J. Irudayaraj and G. McCarty, *Bio-magn. Res. Technol.* 3 [2005] 1-10.
- [35] P. Dallas, V. Georgakilas, D. Niarchos, P. Komninou, T. Kehagias and D. Petridis, *Nanotechnology* 17 (2006) 2046–2053.
- [36] Z. J. Zhang, X. Y. Chen, B. N. Wang and C. W. Shi, *J. Cryst. Growth* 310 (2008) 5453–5457.
- [37] D. Caruntu, G. Caruntu and C. J. O'Connor, *J. Phys. D: Appl. Phys.* 40 (2007) 5801–5809.
- [38] J. S. Lee, J. M. Cha, H. Y. Yoon, J. K. Lee and Y. K. Kim, *Sci. Rep.* 5 (2015) 12135.
- [39] A. M. Demin, A. G. Pershina, K. V. Nevskaya, L. V. Efimova, N. N. Shchegoleva, M. A. Uimin, D. K. Kuznetsov, V. Y. Shur, V. P. Krasnov and L. M. Ogorodova, *RSC Adv.* 6 (2016) 60196–60199.